

# Relativistic Shock Wave with Degenerate Electrons Trapped in Landau Quantized Magnetic Field: Effect of Non-Thermal Heavy Negative Ion

Apul. N. DEVI<sup>1</sup> and Manoj Kr. Deka<sup>2</sup> and

<sup>1</sup>Center for Applied Mathematics and Computing, Siksha 'O' Anusandhan University, Bhubaneswar-751030, Odisha, India.

<sup>2</sup>Department of Applied Sciences, Gauhati University, Guwahati- 781014, Assam, India

## Article Info

Volume 83

Page Number: 10287 - 10297

Publication Issue:

May - June 2020

## Abstract:

The distribution of the relativistic supersonic shock wave in the quantum plasma is studied in the quantized magnet field of Landau with electrons and non-thermal strong negative ions. The existence of the shock wave in such a plasma is studied by using the traditional theoretical solution of the three-dimensional Plasma equation with degenerate electron-density trapped magnetically in a quantized magnet field, relativistic parameter and in the presence of strong negative ions that vary from thermal equilibrium. The electron's degenerate density and the parameter for magnetic measurement and the relative factor have an extraordinary effect on the kind of propagation in this plasma of supersonic shock waves. The non-thermal negative ion population with normalized negative ion density and history have a profound effect on the amplitude of the shock wave. For any particular degenerate electron density, the simultaneous increase of population of nonthermal negative ion and background normalized negative ion density results in the lowest possible shock wave amplitude whereas, the simultaneous increase of nonthermal population of negative ion, normalized negative ion density, relativistic factor and magnetic field results in the highest possible shock wave amplitude within the chosen set of plasma parameters. The relativistic factor leads the height of the shock wave and decreases with a relativistic effect that grows irrespective of any changes in other plasma parameters. A comprehensive comparative analysis is carried out on the function of each leading parameter in the amplitude of the shock wave.

**Keywords:** Electrons Trapped, Non-thermal Heavy Negative Ion, Relativistic plasma, Shock Wave

## Article History

Article Received: 19 November 2019

Revised: 27 January 2020

Accepted: 24 February 2020

Publication: 18 May 2020

## 1 Introduction

Both classical structures and quantum shocks have drawn many researchers worldwide, due to their possible application both in industry and in laboratories. In the study of localized electrostatic oscillations in the astrophysical and laboratory plasma system both, degenerated plasmas containing positive and negative ions, in particular pair-ion or multi-ions[1]. Negative ions have been well

examined in many ionospheric layers, in the cometary environment, in plasma reactors and in laboratory experimentations. Within such plasma

environment, both solitary and shockwave phenomena are well explored[2], [3]. For example, in quantum plasma Misra and Ghosh investigated a sonic magnet shock like structures with dissipation in consideration of spiral alignment and quantum tunnelling effect, and concluded that in a given

quantum plasma context, both oscillatory and stationary shock structures are possible[4], [5]. In a recent study researchers studied shock structures with heavy elements in relativistic quantum plasma and found that monotonic shock structure is possible in the presence of a low electron density in the ultrasound regime while the amplitude of the shock waves decreases in the increasing density of heavy elements. The same study also states that the solitonic hump decreases with the decreasing Bohm potential in non-relativistic and ultra-relativistic situations[6], [7]. Eliason and Shukla recorded the shock wave formation with relativistic electron degeneration and concluded that phase speed in the nonlinear waves increases as the amplitude of the nonlinear waves and shocks increases. Sahu and Misra have noted magnetohydrodynamic shocking structures in quantum plasma with the effect of an interchange and have found that the force of exchange correlations is often dominant instead of pressure gradient and others, and the shock wave can turn from monotonic to oscillatory, with viscosity and diffusiveness[8], [9]. Researcher noted the properties of a quantum plasma with stationary heavy ion shock wave and found that the basic properties of shock wave conditions for non-planar geometry are being substantially altered compared with planar geometry. In an interesting paper, Hossen and Mamun studied the co-existence of alone shock structures in cryogenic quantum plasma and concluded that the dissipation effect which results in the ion acoustic shockwave is due to a strong correlation between cold ions, apart from modifying the basic characteristics of solitary and shock structures[10]. Scientists have examined the formation shock wave of thick plasmas that degenerate and found that shock wave potential increases dramatically, whereas electrons are seen as ultra-relativistic, as non-relativistic as non-relativist and degenerate electrons and ions. The Mamun and Shukla studied non-planar ion acoustic shock waves, and concluded that the height of the shock wave potential is proportional to the square root of the ion

mass at non-relativistic and ultra-relativist stages, while the height of the shock wave potentials is inversely relative to the charged status of the ionic species. Besides this, they also found that the shock height is proportional to the third electron density at the low relative limit while the shock wave's amplitude is proportional to the sixth electron power at the ultra-relativistic limit. Researchers have performed an investigation into the properties of shock waves within the plasma of quantum electron positrons and found that the frequency and steepness of the quantum shock wave decline with the quantum potential. Hussain and Akhtar, on the other hand, have investigated the collisional effect on negative ion-quantum plasma in a recent study and observed a damp K-dV solitary wave with decreases of amplitude (width) with an increasing frequency of collisions. The modulation instability of degenerated ion acoustic waves with negative ions, Tie-Lu et al. have investigated and concluded that there is a clear impact on instability both in a weak and ultra-relative limit on the temperature and density ratio of negative to positive ion and the effect of degeneration. Akhtar and Hussain in another report, observed the shock wave propagation in degenerate dense plasmas with negative ions and they confirmed the existence of compressive and rarefactive shock for a value above and below quantum diffraction parameter. During the degeneration of plasma with oxygen pairs of ions plasma, Michael et al observed shock structure and found that shock intensity increases as the spectral index of the distributed electrons and even with the viscous ion positive oxygen increases. Researchers who studied the propagation of solitary and shockwaves on a plasma with a multi-ion dusty degenerative effect, found that both degenerated electron pressure and multi-ion pressure along with dust densities and charge have a major impact on the power of electrostatic waves in those plasmas. Researchers reported on non-planar solitary wave in negative plasma ion degenerate and found a patent effect on the phase velocity and solitons structure on

the quantum diffraction dimensions, positive / negative ion temperature, and degenerate density of electron. In the final study, Akbari-Moghanjoughi studied the properties of a positive / negative ion plasma degenerating shock wave, which resulted in both compression and rare active shock waves propagating in such a plasma. Throughout this paper the properties of the shock wave in the presence of Landau quantization were discussed. This is extremely significant from a spatial and astrophysical plasma perspective since non-linear shock structures are regarded as one of the principal sources of energy transfer in astrophysical conditions.

## 2 Theoretical Formulation

To research the nonlinear distribution of IA shock waves in relativistic plasma, this paper considers a

collision less magnetized plasma with relativistic Fermi trapped ions. For this method, the basic mathematical expressions governed by the continuity, momentum and pressure equations are as follows;

$$\frac{\partial n_i}{\partial t} + \nabla \cdot (n_i \mathbf{v}_i) = 0$$

$$\left( \frac{\partial}{\partial t} + \mathbf{v}_i \cdot \nabla \right) (\gamma_i \mathbf{v}_i) = -\frac{Z_i q_i}{m_i} \nabla \phi - \frac{\nabla p_i}{m_i n_i} - \frac{\mathbf{v}_i \times \mathbf{B}_0}{c} + \mu_i \nabla^2 \mathbf{v}_i$$

$$\nabla^2 \phi = 4\pi e (n_e - Z_i n_i + Z_n n_n)$$

Researchers have adopted techniques similar to those used in Tsintsadze for Landau for quantified magnetic fields to achieve the electron density for these plasmas; and researchers have found that standard electron density is

$$N_e = \frac{n_e}{n_{e0}} = \frac{3}{2} \frac{1}{\varepsilon_R^2} \left\{ \left( \eta \varepsilon_R^2 \sqrt{1 - \varepsilon_R^2} + \frac{3}{2} (1 - \varepsilon_R^2 - \eta \varepsilon_R^2)^{3/2} \right) + \left( \frac{\eta \varepsilon_R^2}{\sqrt{1 - \varepsilon_R^2}} + \frac{9}{2} \sqrt{1 - \varepsilon_R^2 - \eta \varepsilon_R^2} \right) \phi + \left( \frac{\eta \varepsilon_R^4}{2\sqrt{1 - \varepsilon_R^2} (\varepsilon_R^2 - 1)} + \frac{9}{4} \frac{\sqrt{1 - \varepsilon_R^2 - \eta \varepsilon_R^2} (-2 + \varepsilon_R^2 + \eta \varepsilon_R^2)}{(-1 + \varepsilon_R^2 + \eta \varepsilon_R^2)} \right) \phi^2 \right\} \quad \text{-----(4)}$$

where  $\eta = \frac{2\hbar \omega_{ce}}{m_e c^4}$  shows Landau diamagnetism

effect,  $\varepsilon_R = \frac{m_e c^2}{\mu_e}$  displays the relationship between

the rest mass energy of relativistic electron and the total chemical potential, where  $\mu_e = \varepsilon_{Fe} + m_e c^2$  is the sum of energy from the Fermi and the rest of energy from the mass. The expression  $\varepsilon_{Fe} = \frac{\hbar^2}{2m_e} (3\pi^2 n_{e0})^{2/3}$

is for the Fermi energy and  $\omega_{ce}$  is the cyclotron

frequency of the electrons. The physical quantities  $n_i$ ,  $\mathbf{v}_i$  and  $m_i$  respectively, denote positive ions density, velocity and mass respectively with  $Z_p = +e$ . The relativistic factor is  $\gamma_i = 1 + (v_i^2/2c^2)$ , where  $c$  is the velocity of light. The adiabatic state equation is given for positive ions  $p_i/p_{i0} = (n_i/n_{i0})^\gamma = N_i^\gamma$ , where  $p_{i0} = n_{i0} \kappa_B T_i$ , and  $\gamma (=5/3)$  is the 3D geometry adiabatic index. Therefore, the following standard series of equations (1)-(4) are obtained:

$$\frac{\partial N_i}{\partial T} + \nabla \cdot (N_i \mathbf{V}_i) = 0 \quad \text{----- (5)}$$

$$N_i^{1/3} \frac{\partial (\gamma_i \mathbf{V}_i)}{\partial T} + N_i^{1/3} \mathbf{V}_i \cdot \nabla (\gamma_i \mathbf{V}_i) = -N_i^{1/3} \nabla \phi - \frac{5\sigma_i \nabla N_i}{3} - \mathbf{V}_i \times \boldsymbol{\Omega}_i + \rho N_i^{1/3} \nabla^2 (\mathbf{V}_i) \quad \text{----- (6)}$$

$$\nabla^2 \phi = \mu_e N_e - N_i + \mu_n N_n \quad \text{----- (7)}$$

Where,  $N_i, V_i$  Denote standardized ion density and ion velocity, respectively.  $N_i$  is standardised by equilibrium value  $n_{i0}$  and  $V_i$  by  $C_i (\kappa_B T_i / m_i)^{1/2}$ .  $\phi$  is wave potential standardized by  $\kappa_B T_i \phi / e$ , the time variable  $T$  is standardized by  $\omega_{pi} = (4\pi n_{i0} e^2 / m_i)^{1/2}$  the space variables are standardised by  $C_i / \omega_{pi}$  which gives us  $\omega_{pi} \lambda_d = c_i$ , together with

$\rho = \mu_i / \omega_{pi} \lambda_D^2$ , that is kinematic viscosity of Debye length,  $\lambda_D = (\kappa_B T / 4\pi n_{i0} e^2)^{1/2}$ . Here,  $\mu_e = n_{e0} / n_{i0}$ ,  $\mu_n = n_{n0} / n_{i0}$ ,  $\rho = \mu_i / \omega_{pi} \lambda_D^2$ ,  $\sigma_i = T_i / T_e$ , where  $T_i, T_e$  Positive ion and electron temperatures, respectively and  $\Omega_i = e B_0 / m_i c \omega_{pi}$  is well-defined as an ion gyro-frequency.

The non-thermal negative ion is expressed by

$$N_n = \left\{ 1 + \beta_n \sigma_n \phi + \beta_n (\sigma_n \phi)^2 \right\} \exp(\sigma \phi), \quad \beta_n = \frac{4\alpha_n}{1 + 3\alpha_n}, \quad \sigma_n = \frac{T_n}{T_e}$$

### 3. Evolution Equation of Relativistic Plasmas

The above sequence of Eqs (5) – (7) is used to add the following extension coordinates to obtain the equation of 3D Burgers.

$$\xi = \varepsilon (X - \lambda T), \quad \eta = \varepsilon Y, \quad \zeta = \varepsilon Z, \quad \tau = \varepsilon^2 T, \quad \rho = \varepsilon^{1/2} \rho_0 \quad \text{----- (8)}$$

Where  $\lambda$  is standardized phase velocity.  $N_i, V_i$  and  $\phi$  etc. are extended in power series of  $\varepsilon$  as

$$N_i = 1 + \sum_{j=1}^{\infty} \varepsilon^j N_i^{(j)}, \quad \phi = \sum_{j=1}^{\infty} \varepsilon^j \phi^{(j)}, \quad V_k = V_{i0} + \sum_{j=1}^{\infty} \varepsilon^j V_k^{(j)}, \quad V_{\phi,z} = \sum_{j=3, \ell, k=1}^{\infty} \varepsilon^j V_{\phi,z}^{(k)} \quad \text{----- (9)}$$

The researchers can model the first order equation by (11) and (12) in equations (6)-(10).

$$N_p^{(1)} = a \phi^{(1)}, \quad V_p^{(1)} = w a \phi^{(1)}, \quad w = \lambda - V_0, \quad a = (w^2 \gamma_1 - 5 \sigma_p / 3)^{-1} \quad \text{----- (10)}$$

$$\lambda = \frac{\gamma_1 V_0 \pm \sqrt{\gamma_1^2 V_0^2 + \gamma_1 p}}{\gamma_1} \quad \text{----- (11)}$$

$$\gamma_1 = (1 + 1.5 \gamma^2), \quad \gamma = V_0 / c, \quad p = 5 \sigma_p / 3 + \left\{ (1 - \beta_e) \mu_e + (1 + \beta_n) \mu_n \sigma_n \right\}^{-1} - \gamma_1 V_0^2$$

Similarly, the equations in the second order are modelled as, by matching the x, y and Z equations components (5) – (7),

$$\frac{\partial N_i^{(1)}}{\partial \tau} - w \frac{\partial N_i^{(2)}}{\partial \xi} + \frac{\partial V_{ik}^{(2)}}{\partial \xi} + \frac{\partial (N_i^{(1)} V_{ik}^{(1)})}{\partial \xi} + \frac{\partial V_{\psi}^{(1)}}{\partial \eta} + \frac{\partial V_{\xi}^{(1)}}{\partial \zeta} = 0 \quad \text{----- (12)}$$

$$\begin{aligned} \gamma_1 \frac{\partial V_{ik}^{(1)}}{\partial \tau} - w \gamma_2 \frac{\partial V_{ik}^{(1)^2}}{\partial \xi} - w \gamma_1 \frac{\partial V_{ik}^{(2)}}{\partial \xi} + \gamma_1 V_{ik}^{(1)} \frac{\partial V_{ik}^{(1)}}{\partial \xi} - \frac{w}{3} \gamma_1 N_i^{(1)} \frac{\partial V_{ik}^{(1)}}{\partial \xi} \\ + \frac{\partial \phi^{(2)}}{\partial \xi} + \frac{1}{3} N_i^{(1)} \frac{\partial \phi^{(1)}}{\partial \xi} + \frac{5}{3} \sigma_i \frac{\partial N_i^{(2)}}{\partial \xi} - \rho_0 \frac{\partial^2 V_{ik}^{(1)}}{\partial \xi^2} = 0 \end{aligned} \quad \text{----- (13)}$$

$$\frac{\partial}{\partial \xi} \left( \frac{\partial V_{\psi}}{\partial \eta} \right) + \frac{\partial}{\partial \xi} \left( \frac{\partial V_{\xi}}{\partial \zeta} \right) = \frac{1}{w} \left( 1 + \frac{5}{3} \sigma_i \alpha \right) \left\{ \frac{\partial^2 \phi}{\partial \zeta^2} + \frac{\partial^2 \phi}{\partial \eta^2} \right\} \quad \text{----- (14)}$$

$$\frac{\partial N_i^{(2)}}{\partial \xi} = (\alpha_1 \mu_s + (\alpha_n + 1) \mu_n \sigma) \frac{\partial \phi^{(2)}}{\partial \xi} + (2 \mu_s \alpha_2 + (4 \alpha_n + 1) \mu_n \sigma^2) \phi^{(1)} \frac{\partial \phi^{(1)}}{\partial \xi} \quad \text{----- (15)}$$

$$\text{Where, } \alpha_1 = \frac{3}{2} \eta \frac{1}{\varepsilon_R^3} \left\{ \frac{\varepsilon_R^2}{\sqrt{1 - \varepsilon_R^2}} + \frac{9}{2\eta} \sqrt{1 - \varepsilon_R^2 - \eta \varepsilon_R^2} \right\}$$

$$\alpha_2 = \frac{3}{2} \eta \frac{1}{\varepsilon_R^3} \left\{ \frac{\varepsilon_R^4}{2\sqrt{1 - \varepsilon_R^2} (\varepsilon_R^2 - 1)} + \frac{9}{4\eta} \frac{\sqrt{1 - \varepsilon_R^2 - \eta \varepsilon_R^2} (-2 + \varepsilon_R^2 + \eta \varepsilon_R^2)}{(-1 + \varepsilon_R^2 + \eta \varepsilon_R^2)} \right\}$$

The final 3D-Burgers' equation describing the shock wave production is now obtained by making mathematical calculations by means of equations (12) - (15) along with equations (10) & (11).

$$\frac{\partial}{\partial \xi} \left( \frac{\partial \phi^{(1)}}{\partial \tau} + A \phi^{(1)} \frac{\partial \phi^{(1)}}{\partial \xi} - B \frac{\partial^2 \phi^{(1)}}{\partial \xi^2} \right) + C \left( \frac{\partial^2 \phi}{\partial \zeta^2} + \frac{\partial^2 \phi}{\partial \eta^2} \right) = 0$$

$$\text{Where } A = \frac{(8\gamma_1 w^2 \alpha_1^2 - w^3 \alpha_1^2 \gamma_2 \delta + \alpha_1) + (2\mu_s \alpha_2 + (4\alpha_n + 1) \mu_n \sigma^2) (5\sigma_i - 3w^2 \gamma_1)}{6\gamma_1 w \alpha_1}$$

$$B = \frac{\rho_{p0}}{2\gamma_1}, \quad C = \frac{1}{2w} \left( \frac{1}{\alpha_1} + \frac{5}{3} \sigma_i \right)$$

$\phi_m = \{U(1 - C(1 - l^2))\} / Al^2$  and  $\omega = 2Bl^3 / \{U(1 - C(1 - l^2))\}$  are the maximum amplitude and thickness of the

The 3D-Burgers' stationary solution equation (16) as

$$\phi^{(1)} = \phi_m \left\{ 1 - \tanh \left( \frac{\chi}{\omega} \right) \right\}$$

shock wave, with  $l$  representing the angle direction cosines formed by the propagating x-axis shock wave and  $U$  represent velocity.

#### 4 Result and Discussion

Where,

From the analytical solution, in the context of various physical conditions, (18) we discuss the existence and properties of the solitary wave distribution. Here the loaded particle densities in plasma have been taken into consideration as  $1026-29 \text{ cc}$ , the ambient magnetic field as  $109 \sim$

$1012 \text{ Gauss}$ , the temperature of Fermi being within  $3.6277 \times 10^7 \text{ K}$  [31-35] for certain plasma parameters. We also found Helium positive ions in our entire analytical study because of the plasma system in abundance.

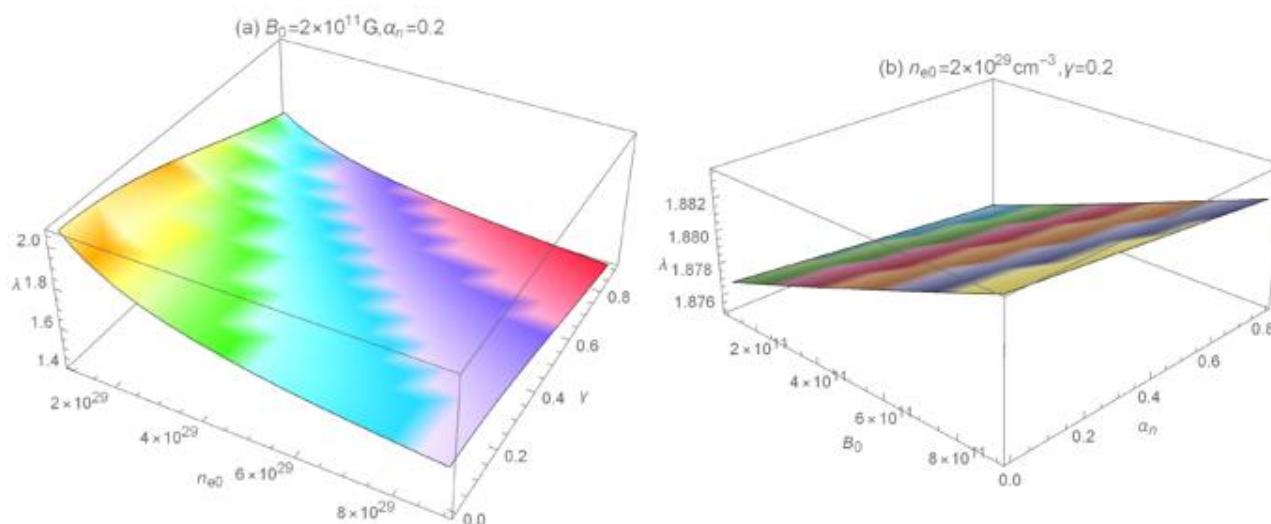


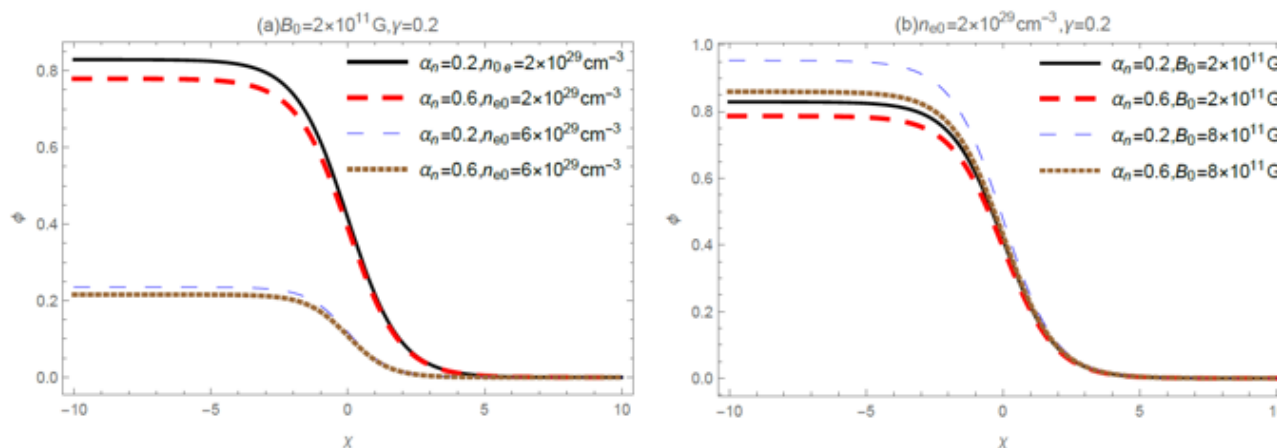
**Figure 1: (a) Variation in the normalized phase velocity of the relative factor shockwave, with different degenerated densities of electron. (b) Variation of plasma system nonlinearity with non-thermal negative ion parameters, at different degenerate electron density.**

The variance of the normalised phase velocity with the relative factor for different degenerate electron density in a particular magnetic field is defined in Figure 1(a). From the graph, the phase velocity decreases and even with increasing the relativistic factor the phase velocity decreases as we proceed to increase the degenerate electron density. This may be because as the relativistic factor increases, the faster plasma particles will have a greater and frequent interaction or collision probability and also with increasing background plasma density, It would increase the likelihood of collision, which will greatly reduce the plasma system's average phase speed. The phase varying speeds with magnetic field strength as well as the non-thermal population of heavy negative ions are defined in Figure 1(b). As the magnetic field's function is to confine the plasma species in its direction and in this situation, the principle behind this graph is the other plasma particles have a better and greater chance of interaction with the magnetized plasma species

instead of non-magnetized randomized motion of the plasma species. This exactly happens in figure 1(b). As the figure shows, the magnetic field is growing, the phase speed increases due to the conduit movement of the plasma degenerate electrons along the magnetic field which would contribute to the average phase velocity enhancement instead of random movement of the degenerate electrons where the average phase velocity can be expected to be less in the absence of magnetic field. In comparison, the average phase velocity is decreased at any intensity in the magnetic field by increasing the non-thermal strong negative ion population. It goes without saying that with the heavy negative ions being more and more non-thermal, contact with other plasma particles and negative ions being the strongest species would still reduce the phase speed. Compared to the variation in the phase speed with the magnetic field and non-thermal populations of the heavy ions, the rate of increase is greater than the rate of

reduction of the phase velocity  $\alpha_n$  with an increase on the magnetic field. This is primarily due to the negative ions and as it deviates more and more from the thermal behaviour (with increasing non-thermal

parameter), the probability of interaction with other plasma species decreases which is the result of lower rate of decrease of phase speed with growing non-thermal population of negative ion.



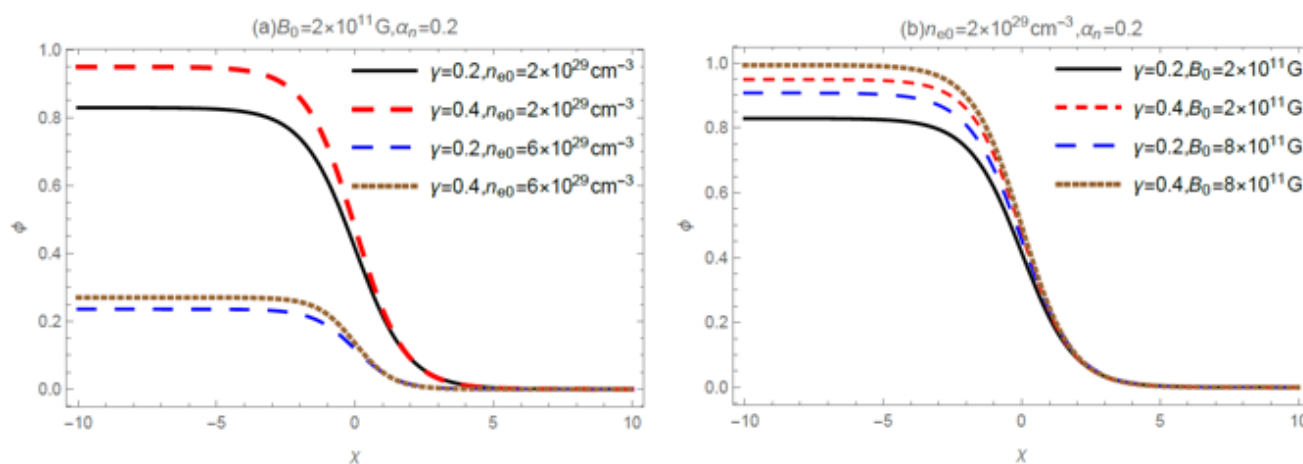
**Figure 2: (a) Shockwave Potential variance with non-thermal negative ion parameters  $\alpha_n$ , at different degenerate electron density  $n_{e0}$ , here the other plasma parameter are considered as  $B_0 = 2 \times 10^{11} \text{ G}$  and,  $\gamma = 0.2$  (b) Shock-wave potential variance with non-thermal ion negative parameter  $\alpha_n$  at different magnetic field  $B_0$ , here the other plasma parameter are considered as  $n_{e0} = 2 \times 10^{29} \text{ cm}^{-3}$  and,  $\gamma = 0.2$ .**

Figure 2(a) describes the distribution of shocks with a combined effect of negative ion non-thermal parameter and degenerate electron density for the magnetic field strength and relative strength value of a fixed values. The shock amplitude decreases, as can be seen from the diagram, with increasingly low electron density  $\alpha_n$ . For this analysis the solution for the dynamic evolution equation shows that the ultimate shock wave amplitude depends primarily on the increase / decrease of nonlinearity. So, the average shock height decreases (increases) as nonlinearity increases (decreases). With the rising of the electron density, the plasma system becomes very nonlinear, thus reducing shock potential. The increase in the non-thermal negative ion population, which is further deviation from non-thermally, further increases the non-linearity of the plasma medium and thus decreases the amplitude with an increased rating. Around the same time, with increased degenerate electron densities, shock height decreases dramatically while the shock wave potential reduction rate with, is higher when the

electron density is lower than when the electron density is higher. This is because with negative ions being the heaviest species, the deviation of the negative ions from non-thermal behaviour will have lesser impact on the nonlinearity of plasma system than impact on non-linearity due to increment in the dominant degenerating electron density. Thus, though the overall effect of increasing non-thermal population at any electron density will result in an enhancement of the overall non-linearity (hence lower shock potential), the increase in the electron density will have a higher impact on non-linearity. Thus, it can be concluded that the addition of non-thermal population of negative ion at lower electron density will have lower nonlinearity than compared to addition of non-thermal population of negative ion at higher electron density due to the dominant effect of degenerate electrons. Thus, the rate of decrease of wave potential is more, on addition of non-thermal population of negative ion at lower electron density than due to the addition of non-thermal population of negative ions at higher electron density. Figure 2(b)

shows the combined effect of non-thermal population of negative ion and magnetic field on shock wave potential for fixed value of degenerate electron density and relativistic factor. As seen from the graph, the shock height decreases with increasing the non-thermal population of negative ions but with increasing magnetic field strength, the shock potential increases as, we know the role magnetic field is to streamline the flow of the plasma species which in turn reduce the nonlinearity and hence a greater potential of shock wave. Alternatively, if we increase the non-thermal ion population at higher magnetic field (Brown Dotted Curve), the shock wave potential decreases significantly compared to

the rate of decrement of potential of shock wave at low magnetic field with the increase of non-thermal negative ion population (Red Thick Dashed Curve). This may be possible, as with increasing magnetic field plasma species are bound to move in a more ductus way and if in such condition non-thermal negative ion population is increased, the overall possibility of effective interaction increases than that compared to the random motion of the plasma species. This in turn increases the nonlinearity of plasma species and hence we see further reduction in shock wave potential.



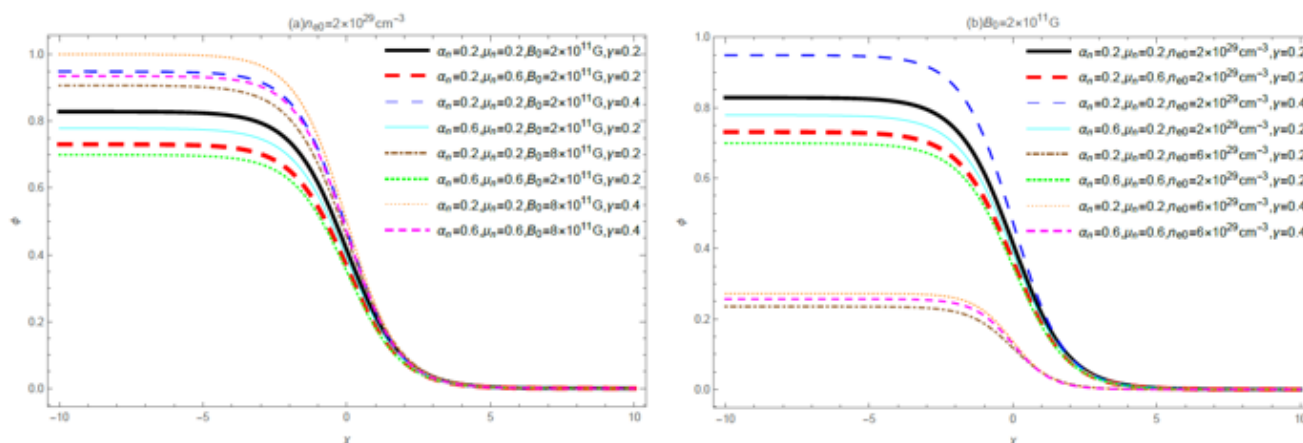
**Fig.3 (a) Shock wave potential variation with relativistic factor  $\gamma$  at divergent degenerate electron density  $n_{e0}$ , here the other plasma parameter are considered as  $B_0 = 2 \times 10^{11} G$  and,  $\alpha_n = 0.2$  (b) Shock wave potential variation with relativistic factor  $\gamma$  at different magnetic field, here the other plasma parameter are considered as  $n_{e0} = 2 \times 10^{29} cm^{-3}$  and,  $\alpha_n = 0.2$ .**

Figure 3 (a) describes relativistic factor effect and regenerate electron density on shock strength. The shock potential rises (diminishes) with the relativistic factor (degenerate electron density) which can be easily understood through above topic. The combination of relativistic and magnetic field effects on the shock height as shown in Figure 3(b) is now the most fascinating fact. The graph shows that an increase in the value of relativistic factor, the shock potential increases for a particular magnetic field. This is because, as  $\gamma$  increases, the velocity of the plasma electrons and ions increases and it is well

known that for a magnetized plasma the rate of confining of plasma particles along magnetic field is higher for the faster particles and as a result, the nonlinearity tends to decrease due to streamline motion of the plasma species which in turn increases the shock wave potential (Red Thick Dashed Curve). Alternatively, if we increase magnetic field alone (Blue Thin Dashed Curve), the shock wave potential increases. This is due to the magnetic field which simplifies the flow of plasma particles, which reduces nonlinearity and hence the shock wave's greater potential. However if we simultaneously

increase the relativistic factor and the magnetic field (Figure 3(b)), the shock wave potential is maximum in plasma. This is because the faster and the higher the speed and magnetic field, the better is the streamline flow of the plasma particle which results

in the least possible non-linearity amongst the chosen combination of the plasma parameter and hence the highest is the shock wave potential (the uppermost Brown Dotted curve).



**Figure 4: (a) Combined effect of relativistic factor  $\gamma$ , magnetic field  $B_0$ , negative ion non-thermal parameter  $\alpha_n$  and standardised negative ion density  $\mu_n$  for a constant degenerate electron density  $n_{e0}$ , on shock wave potential (b) Relativistic factor  $\gamma$  combined effect, degenerate electron density  $n_{e0}$ , non-thermal parameter of negative ion  $\alpha_n$  and normalized negative ion density  $\mu_n$  for a fixed magnetic field  $B_0$ , on shock wave potential.**

In figure 4 (a) and we place a comparative study of the shock wave potential variation with the relativistic factor  $\gamma$ , non-thermal negative ion population  $\alpha_n$ , background negative ion density  $\mu_n$  and magnetic field  $B_0$  for a fixed value of degenerate electron density  $n_{e0}$  and figure 4 (b) the same comparative study at a fixed value of magnetic field  $B_0$  with the relativistic factor  $\gamma$ , non-thermal negative ion population  $\alpha_n$ , background negative ion density  $\mu_n$  and degenerate electron density  $n_{e0}$  is placed. As seen from the figure 4(a), the present plasma system shows the lowest possible values of shock wave potential when the background negative ion density and non-thermal negative ion population increases simultaneously for a fixed value of  $B_0$  and  $\gamma$  (Green Dotted Curve) and the highest possible shock wave potential is seen when both  $\gamma$  and  $B_0$  increases simultaneously. This is very interesting. If

we study the physics behind it, we see that when the non-thermal negative ion population and background negative ion density increases simultaneously, the nonlinear behaviour of the plasma medium increases noticeably due to the deviation of the plasma system from non-thermal and this deviation from non-thermal increases further as we increase the population of these two species and Therefore the least potential for shock among the plasma parameters is selected. Alternatively, at the same time the shock potential is greater (Uppermost Curve) with the change in the magnetic field and relativistic factor. This is because the plasma mechanism is not the least nonlinear due to two reasons, if both the magnetic and relativistic factors simultaneously increase, the increase of a magnetic field streamlines the plasma-flow and thus decreases the non-linearity of the behaviour, and secondly, the increase in the relativistic factor allows plasma electrons and ions to travel through the magnetic field. Thus, the shock potential is greatest when

nonlinearity is greatly reduced, since the maximum wave potential is already addressed as an inverse function of non-linearity for the present plasma networks. Apart from this, the reduction of shock wave potential, with background negative ion density, keeping other parameters fixed (Red Thick Dashed Curve) is more than the reduction of shock wave potential with nonthermal population of negative ions, keeping other plasma parameter fixed (Cyan Thin Solid Curve). On the other hand, if either magnetic field (Brown Dot Dashed Curve) or relativistic factor (Blue Medium Dashed Curve) is increased, the shock wave potential shows an enhancement with relativistic factor than with magnetic field. This may be possible due to higher rate of decrease of nonlinearity involving faster particle (increase in  $\gamma$ ) in a magnetic field. When all the parameters are increased simultaneously, the combined effect of increase of magnetic field and relativistic factor will result in decrease of nonlinearity but the presence of non-thermal population of negative ion and background negative ion density will further enhance the nonlinearity and hence the shock wave potential lies in between (Magenta Small dashed Curve) the shock wave potential arising due to increment in relativistic factor and magnetic field respectively. The other variations of the shock wave described in plot can be understood from the conversation placed above. Same comparative study is carried out for a fixed magnetic field value varying other four plasma parameters i.e.  $n_{e0}$ ,  $\gamma$ ,  $\alpha_n$  and  $\mu_n$  respectively. Here, it can be seen from graph that shock wave potential is the lowest when electron density increases significantly (Brown Dot Dashed Curve) as with increasing electron density the plasma system is expected to behave with highest nonlinearity with other parameters being invariant. Alternatively, with increasing relativistic factor, plasma system nonlinearity is expected to be the least due to the possible reason discussed in the case of above figures and we observe a highest possible shock wave potential. Further, the shock wave potential

decreases with increasing  $\alpha_n$  and  $\mu_n$  also, but the increase of electron density has a greater effect on the reduction of the shock wave potential than compared to additional plasma parameters. The variation of the shock wave potential with other plasma parameter i.e.  $\alpha_n$ ,  $\mu_n$  and  $\gamma$  is prominent when electron density is on the lower side (the upper four curves of the plot) than when the electron density is on the higher side (the extreme three lower curves). Apart from this, the reduction of shock wave potential, with background negative ion density, keeping other parameters fixed (Red Thick Dashed Curve) is more than the reduction of shock wave potential with non-thermal population of negative ions, keeping other plasma parameter fixed (Cyan Thin Solid Curve). Alternatively, shock wave potential further decreases with increasing both  $\alpha_n$  and  $\mu_n$  (Green Dotted Curve), possibly due to further enhancement in the nonlinearity of the plasmas system due to the simultaneous increase of both the parameters. Apart from this the simultaneous increase of  $\alpha_n$ ,  $\mu_n$ ,  $n_{e0}$  and  $\gamma$  will result in further reduction of shock potential (Magenta Small Dashed Curve) than the shock potential arising due to the increase in  $n_{e0}$  and  $\gamma$  for obvious reason and it should be clear from the discussion already put in above paragraph. However, apart from all these parameters, the electron density has the highest impact on the shock wave potential for any combination of physical plasma parameters (e.g. the lowermost Brown Dashed Dotted curve).

## 5. Conclusion

Here we researched the development of a degenerated plasma in a Landau Quantized Relativist supersonic shock wave. With the aid of a three-dimensional (3D) burgers equation the influence of many plasma parameters on the propagation structure of the shock wave is investigated. The magnetic field, the density of electron and the relativist factor have a remarkable effect on both the height of the effect wave and the

phase speed and non-linearity of the plasma medium in this analysis. The relative factor and the magnetic field have an amazing influence on the amplitude of the shock wave when the electron density is small, while the electron density influences the distribution characteristics of the shock waves for a higher range of electron density. If the electron density is on the lower side, so the same pattern of higher electron density but of low growth rate is held, the rate of increase of shock wave potential with magnetic field and relativist factor is higher.

### Acknowledgement

Manoj Kumar Deka from DST-SERB is highly appreciated for the grant received (YSS/2015/001896) for the financial assistance for current research.

### References

1. M. K. Deka and A. N. Dev, "Supersonic Shock Wave with Landau Quantization in a Relativistic Degenerate Plasma\*," *Chinese Phys. Lett.*, 2020, doi: 10.1088/0256-307X/37/1/016101.
2. A. Atteya, E. E. Behery, and W. F. El-Taibany, "Ion acoustic shock waves in a degenerate relativistic plasma with nuclei of heavy elements," *Eur. Phys. J. Plus*, 2017, doi: 10.1140/epjp/i2017-11367-2.
3. O. Zanotti and M. Dumbser, "High order numerical simulations of the Richtmyer-Meshkov instability in a relativistic fluid," *Phys. Fluids*, 2015, doi: 10.1063/1.4926585.
4. H. J. Xu, J. Zhao, Y. Feng, and F. Wang, "Complications in the interpretation of the charge-asymmetry-dependent  $\pi$  flow for the chiral magnetic wave," *Phys. Rev. C*, 2020, doi: 10.1103/PhysRevC.101.014913.
5. R. Denra, S. Paul, U. Ghosh, and S. Sarkar, "Nonlinear dust-acoustic wave propagation in a Lorentzian dusty plasma in presence of negative ions," *J. Plasma Phys.*, 2018, doi: 10.1017/S0022377818001034.
6. S. Eliezer, Z. Henis, N. Nissim, S. V. Pinhasi, and J. M. Martinez Val, "Introducing a two temperature plasma ignition in inertial confined targets under the effect of relativistic shock waves: The case of DT and pB11," *Laser Part. Beams*, 2015, doi: 10.1017/S0263034615000701.
7. M. R. Hossen, M. A. Hossen, S. Sultana, and A. A. Mamun, "Modeling of modified ion-acoustic shock waves in a relativistic electron degenerate multi-ion plasma for higher order nonlinearity," *Astrophys. Space Sci.*, 2015, doi: 10.1007/s10509-015-2278-7.
8. R. Denra, S. Paul, and S. Sarkar, "Characteristics of nonlinear dust acoustic waves in a Lorentzian dusty plasma with effect of adiabatic and nonadiabatic grain charge fluctuation," *AIP Adv.*, 2016, doi: 10.1063/1.4972520.
9. X. L. Zhao, G. L. Ma, and Y. G. Ma, "Novel mechanism for electric quadrupole moment generation in relativistic heavy-ion collisions," *Phys. Lett. Sect. B Nucl. Elem. Part. High-Energy Phys.*, 2019, doi: 10.1016/j.physletb.2019.04.002.
10. M. Rybczyński and Z. Włodarczyk, "Fluctuations and clustering of multiplicity in collisions of relativistic ions," *Eur. Phys. J. A*, 2020, doi: 10.1140/epja/s10050-020-00030-1.